J. KAU: Mar. Sci., **vol. 10,** pp. 89-106 (1419 A.H. / 1999 A.D.)

Sedimentology and Geochemistry of The Karan Island Sediments, Arabian Gulf, Saudi Arabia

MOHAMMED H. BASYONI
Faculty of Earth Sciences, King Abdulaziz University, Jeddah, Saudi Arabia

ABSTRACT. Karan island is a coral reef island composed mainly of calcite and aragonite. The island is covered with medium to coarse-grained skeletal and non-skeletal carbonate sands of marine origin and very rare wind blown clay particles. These sediments are characterized by unimodal distribution and well sorted to poorly sorted.

Mineralogical and chemical composition of the Karan island sediments proved that their origin is from the underlying coral reefs.

Introduction

The Karan island is an offshore coral reef island in the Arabian Gulf about 60 km northeast of the city of Jubail (Fig. 1). The island is about 2100 meters long and a maximum width of 640 meters. It is surrounded by an extensive coral reef (Figs. 2&3), and is built on top of the coral reef, where it has a perimeter of about 5.3 km measured at mean high tide, and extended to the northern side of the island (Fig. 2).

The island is covered by medium to very coarse grained sand and consists of reef debris, gastropods, bivalves, and foraminiferal shell fragments. They generally form the major components in the bioclastic sediments, with the association of red and green algae and peloids.

The purpose of this study is to investigate the sedimentological characteristics, mineralogical and geochemical composition of the island sediments. In addition, the relationship between the grain size distribution and the shore transport processes of the island sediments has been emphasized.

Previous Investigations

In recent years, various studies have been carried out on both coastal and island areas of the Arabian Gulf. The Iranian basin is subdivided into two secondary depression – western basin and the central basin. The other side of the Arabian Gulf is called the Ara-

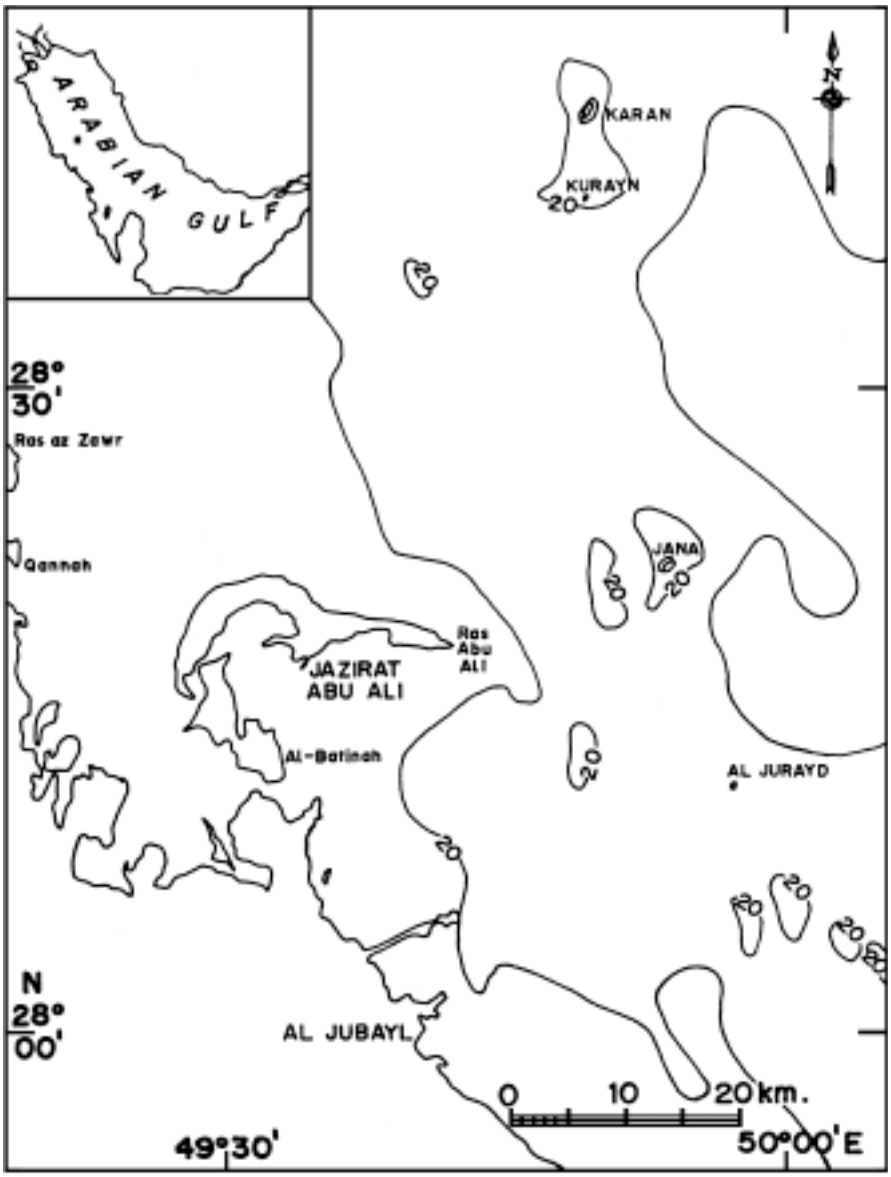

FIG. 1. The location map of the Karan island in the Arabian Gulf (After Al-Mansi *et al.*, 1996).

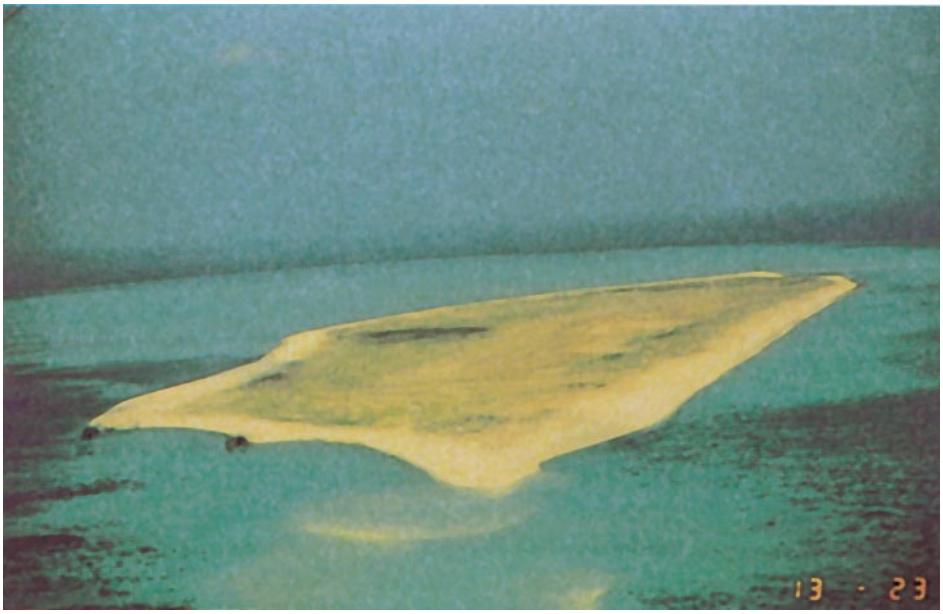

FIG. 2. North east view of the Karan island showing an extensive coral reef surrounding the island.

FIG. 3. South eastern view for the Karan island showing the vegetation of low shrubs of *Suaed* sp., and *Salsola* sp., in the middle of the island. Also of phylum Chrosophyta, along the northern and eastern parts of the island.

bian shallow shelf (or the Arabian Homocline) according to the stress of inclined characters of the Arabian sea floor.

This gentle slope allows a high degree of wave agitation along the Arabian coastlines. Though, contrast with the more classical carbonate shelves sedimentologically and morphologically. Evamy (1973) investigated the precipitation of aragonite and its alteration to calcite on the Trucial Coast of the Arabian Gulf. Purser and Seibold (1973) concluded that the tidal currents are oriented approximately parallel to the axis of the Gulf. Corals are widely spread in the Arabian Gulf as stated by Hughes and Keij (1973). Mc Cave (1978) pointed out that the coarsing trend from the source due to transport along the beach with winnowing out of finer fraction by tidal currents to be progressive. Fryberger *et al.* (1983) drew a map for the types of sediments in the Arabian Gulf. Sirag (1984) outlined the climatological features of Saudi Arabia. Khalaf *et al.* (1984) studied the sedimentological characteristics of the surficial sediments of the Kuwaiti marine environments northern the Arabian Gulf. The calcium carbonate (aragonite and calcite) is largely algal and/or bacterial, and even the strontianite is largely organic in origin (Javor, 1985). Hunter (1986) concluded the physical oceanography of the Arabian Gulf. Milliman (1989) discussed the sea level changes at the past, present, and future depending on fluctuations in the sea, and on the geological stability of the land. Sheppard and Sheppard (1991) studied the coral and coral communities of the Karan island. Basyoni and Al-Mansi (1993) emphasized the grain size significances of the recent reef Eqah island, Red Sea, Saudi Arabia. Al-Mansi *et al.* (1996) studied the seasonal profile changes in exposed beaches in western Arabian Gulf. Basaham and El-Sayed (1998) concluded that the bottom sediments of the Arabian Gulf are composed by biogenic carbonate accumulation and terrigenous material influx.

Geomorphology

Karan island is the largest offshore island near the eastern coast of Al-Jubail. It appeared to the surface during the uplifting of the western side of the Arabian Gulf and sea level changes. The wave erosion on the reef has produced a distinct type of carbonate sand sediments, and resulted from a reworking of the loose sediments by the western north waves similar to the situation in the Eqah island in the Red Sea (Basyoni and Al-Mansi, 1993).

The tidal flat ridges has been raised 0.5 to 1.5 meters above the high sea level (the tidal range is generally less than two meters). The Karan island is protected from the strong waves by reef.

The Karan island is mainly flat and covered by phylum Chrosophyta along the northern and eastern parts of the island. Plants such as *Suaeda* sp. and *Salsola* sp. also grow in the middle of the island in the form of low shrubs (Fig. 3).

Result and Discussion

Grain Size Distribution

Forty six samples were collected mainly from the unconsolidated sediments overlying the consolidated reef limestone in the main island and the adjacent areas (Fig. 4).

The sediments are mostly composed of calcium carbonate; comprising skeletal and non-skeletal grains. The samples were air dried in the laboratory and the grain size of the sediments was determined by sieving for about 15 minutes. Several sieve sizes were used in serial numbers from 2 phi to + 4.5 phi and a pan. All grains smaller than 4.5 phi are referred to as fines.

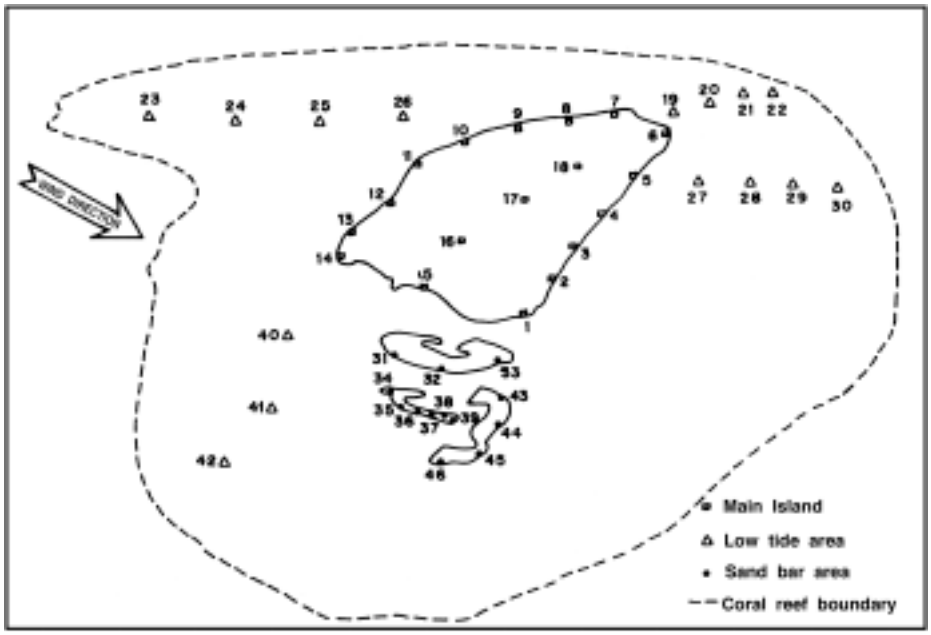

FIG. 4. The wind direction and location of collected samples for Karan island and the surrounding area.

The grain size parameters after Folk and Ward (1957) and Moshrif (1987) and the grain size frequency data of the sediments were represented graphically as histograms and cumulative curves given in Figs. 5A, 5B and 5C. The distribution and significances of grain size parameters of the sediments studied here are shown in Figs. 6A, 6B, 6C and 6D. The histograms constructed for the Karan island sediments (Fig. 5) generally shows unimodal distribution with a dominant modal class falling in the medium sand fraction and in the coarse-grained fraction for the sand bar area. While the sediments in the surrounding shallow area display asymmetric bimodal distribution generally due to the increasing erosion power of waves.

The constructed cumulative curves show two distinctive subpopulation; traction and saltation. The saltation load constitutes the major part of the sediments and mostly poorly sorted for the surrounding shallow area, while the suspension population is very limited and generally of low frequency.

According to the values of grain size parameters obtained and the verbal scale reported by Folk (1968) and summarized graphically in Figs. 6A, 6B, 6C and 6D, the following observations are recorded.

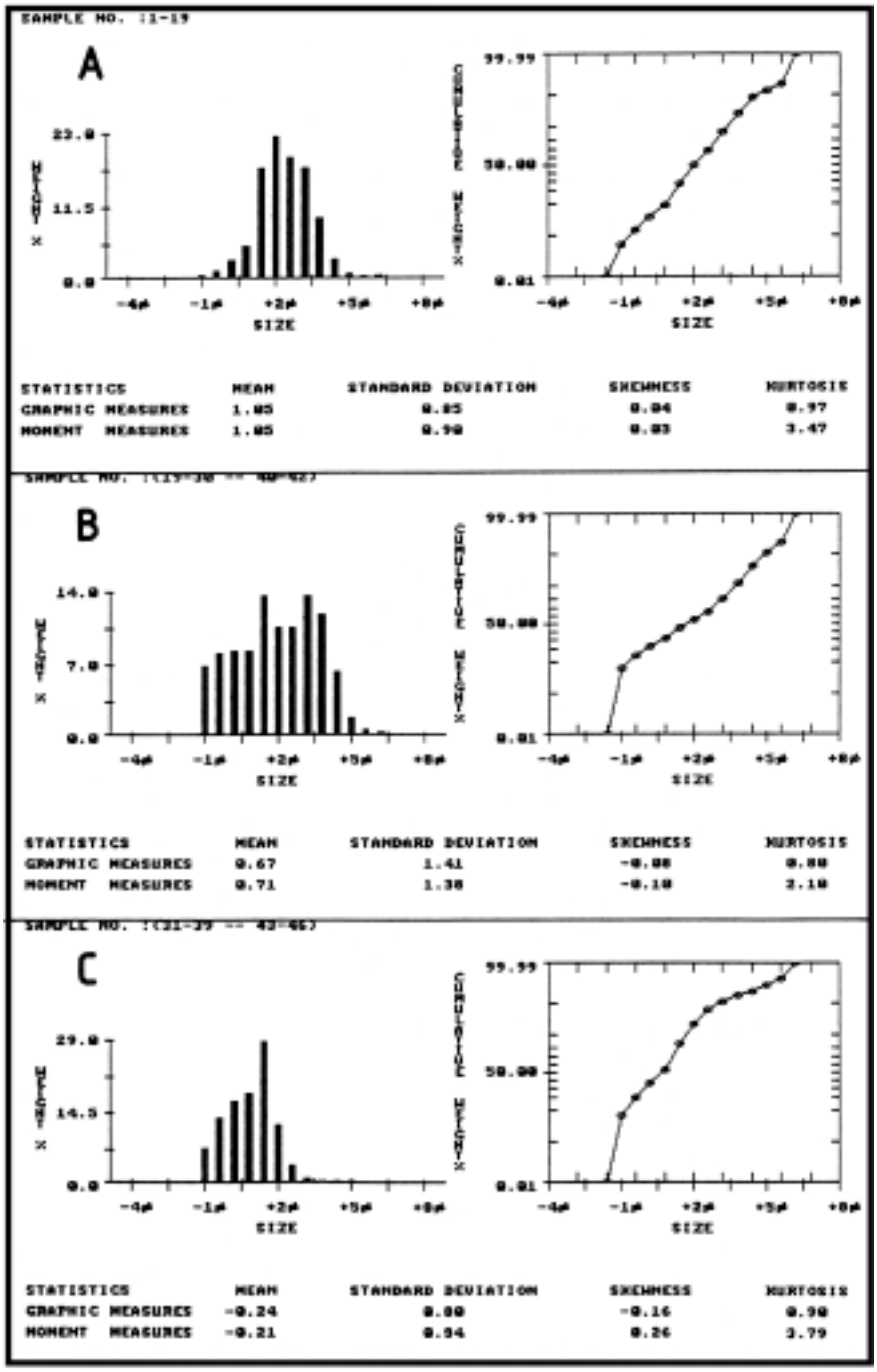

FIG. 5. Average sediments texture parameters for the Karan island (A), the surrounding shallow area, (B) and the sand bar area (C).

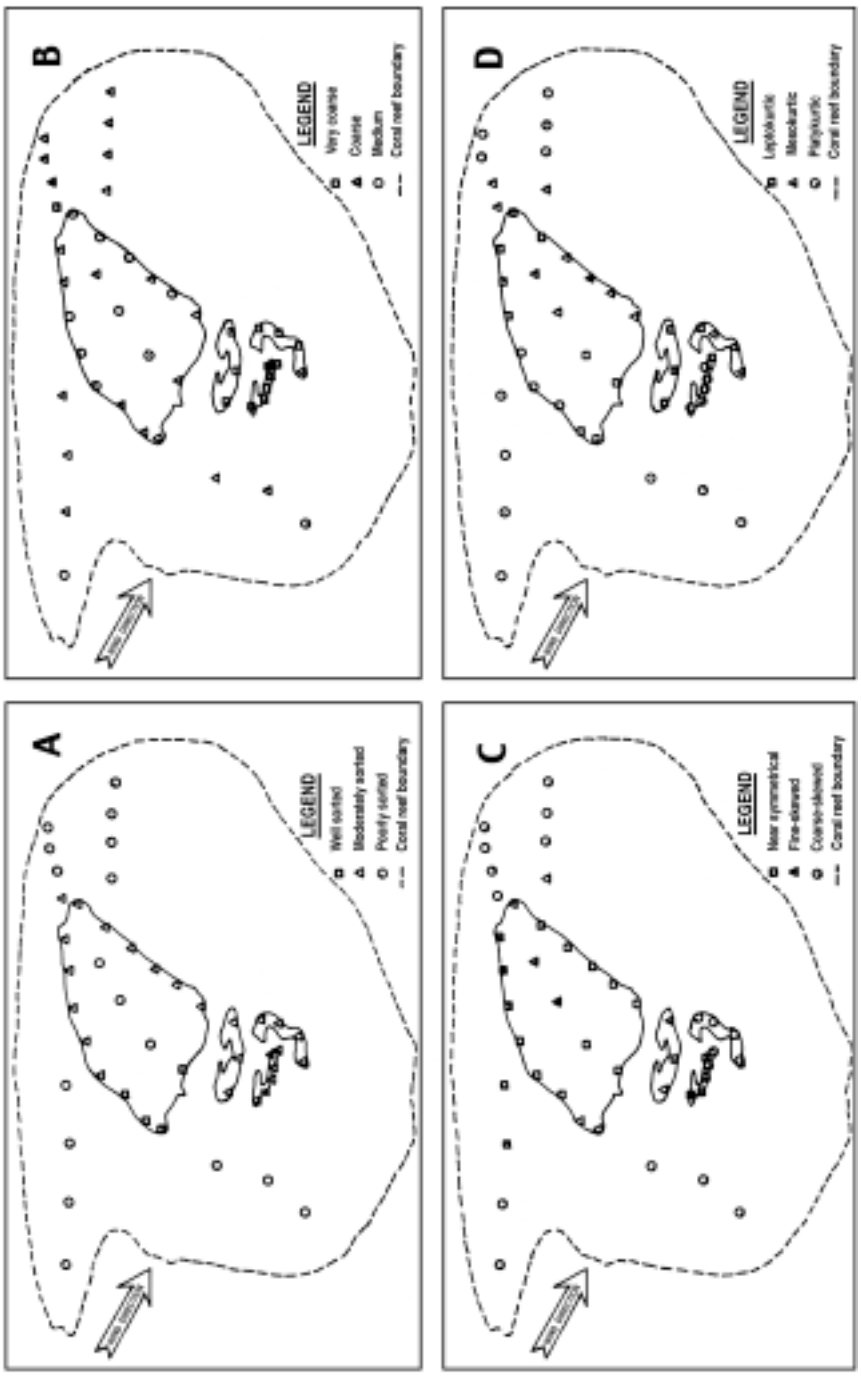

FIG. 6. The distribution of the standard deviation (A), the mean grain size, (B) the skewness, (C) and the kurtosis, (D) of the carbonate sand of Karan island and the surrounding areas.

Mean size

Mean size data indicates that the sediments of the Karan island, are generally oscillate between medium grained and coarse grained, while those of the adjacent shallow areas are mainly coarse grained. A conspicuous very course grained sand is reflected by the sediments in the sand bar area. The finer grain size materials are generally winnowed by the action of the waves and currents.

Standard deviation

The values of standard deviation exhibit pattern fit into the category of poorly sorted for the adjacent shallow area and the central part of the main Karan island. A general moderately sorting is exhibited by the sediments in the beach zone of the island and in the sand bar area. The improvement in sorting is generally related to the energy fluctuations.

The content of dust particles (finer than 0.39 phi) in the sediments is found to be high along the shoreline of the island and being low in the surrounded areas. About 4% to 6.3% dust was found in the main body of the island.

Skewness and kurtosis distribution

Values of graphic skewness show that the Karan island sediments are near symmetrical and fine skewed. In contrast, the surrounding shallow areas have coarse skewed and platy kurtic sediments, whereas the sand bar area exhibits a wide range of skewness and kurtosis values varies from fine skewed to coarse skewed and from leptokurtic to platykurtic. It is evident that the variability in kurtosis is related to the energy change regimes from the shoreline towards the open sea.

Sediment Transportation

The Karan island beach with its gentle slope has an important influence on the shore transport, with an exposed, windward side, and more sheltered leeward margin. Carbonate sand sediments are formed on the reef flat surface covered with mobile coarse particles near the windward margin (including the sand bar areas) and decrease to the direction of south east, however, these are stabilized by vegetation.

The tidal currents of the island tend to follow the axis of the gulf, with slight variable direction tidal currents. The mobile sand blanket is dumped at the confluence of the opposing sets of waves refracted around the reef front to form sand clays. As a result of these physical processes the reef becomes aligned with its long axis parallel to the prevailing wind.

Minerology and Geochemistry

The mineralogical composition of the studied carbonate sediments has been identified by X-ray diffraction analysis. The bulk mineral components and the relative abundance of each mineral have been calculated on the basis of peak high measurements of 100% reflection peak. The data obtained are summarized in Table (1) and some selected ray diffractograms are given in Fig. (7).

TABLE 1. Summary of statistical analysis of major and trace elements, Karan island, KSA.

Variable	Range		Mean	Dispersion				
	Fr	To	X	S	C.V.	Se	Skw	Kurt
Na_2O	.51	1.36	.83	.22	26.95	.03	.09	1.91
CaO	45.71	51.44	48.83	1.23	2.53	.19	– .41	3.02
MgO	1.61	7.16	4.11	1.30	31.59	.20	.57	2.65
Fe_2O_3	.03	.05	.04	.01	19.37	.00	.23	2.22
L.O.I.	44.91	45.69	45.27	.23	.50	.03	.31	2.04
I.R.	.12	.39	.24	.07	26.86	.01	.11	2.13
Sr	390.32	652.88	503.53	64.05	12.72	9.77	.06	2.23
Pb	16.53	35.92	23.99	4.34	18.08	.66	.96	4.08
Cr	11.72	79.95	43.65	19.84	45.45	3.03	– .13	1.72
Zn	6.23	63.95	16.66	9.68	58.13	1.48	2.82	13.85
Co	16.80	117.74	59.05	19.13	32.39	2.92	.33	4.71
Cu	9.25	47.81	19.45	7.75	39.87	1.18	2.15	8.74
Ni	24.12	69.86	41.26	10.71	25.96	1.63	.57	2.77

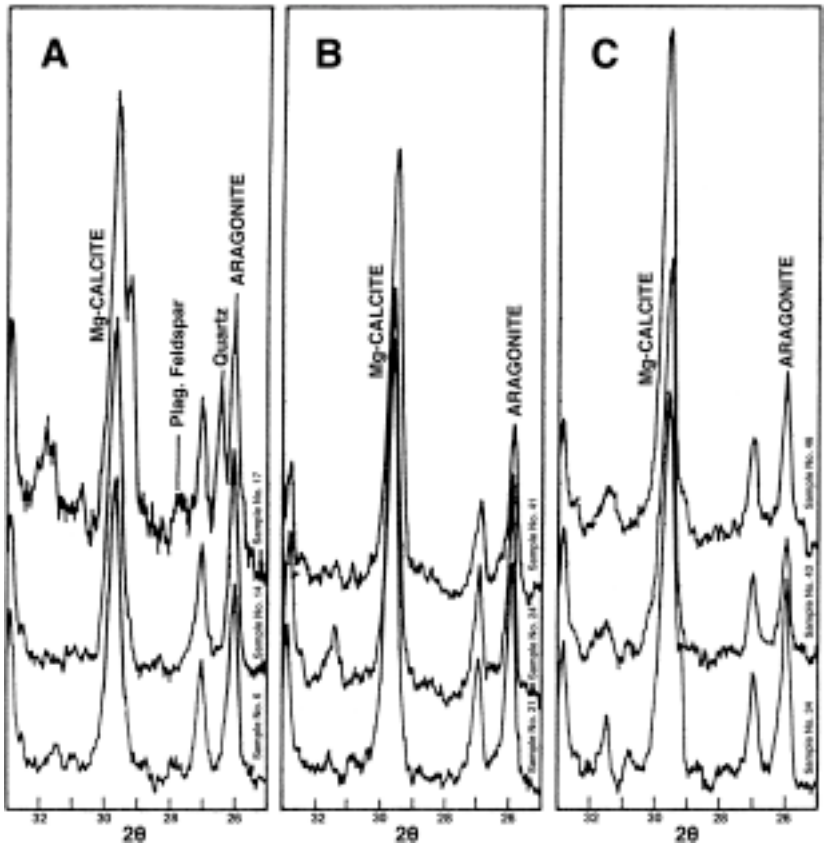

FIG. 7. The x-ray diffraction pattern showing the main reflection of the mineral composing the representative of the main island (A) the low tide (shallow) area, (B) and the sand bar area (C).

In general the total mineral components determined in the studied Karan island sediments and its surroundings include mainly the carbonate minerals, Mg-calcite and aragonite. Detrital minerals quartz and plagioclase feldspars are being recorded as a minor constituents especially in the main island. Mg-calcite recorded here always dominates over aragonite. The detrital minerals were transported by wind as dust and accumulated over the surface of the main island. The recorded calcite in the main island sediments reflects the subaerial exposure of these sediments and diagenetic alteration of metastable Mg-calcite to calcite. The low Mg-calcite in the reef sediments is derived from the coral limestone which surrounded the island by wave erosion.

Concentration of the major oxides (CaO, MgO, Fe_2O_3, Na_2O and K_2O) and trace elements (Sr, Pb, Cr, Zn, Co, Cu and Ni) have been measured in the collected samples, data are presented in Tables (2 and 3). The calculated correlation coefficients between the major oxides, $CaCO_3$, Sr and the acid insoluble residue are listed in Table (4).

Table 2. Chemical analysis shows the major elements percentages in all samples.

Sample no.	Na_2O	K_2O	CaO	MgO	Fe_2O_3	L.I.O.	I.R. %	Total
1	0.53	0.03	50.73	3.45	0.041	44.96	0.25	99.99
2	0.51	0.03	50.86	2.73	0.050	45.05	0.39	99.62
3	0.56	0.03	48.88	3.44	0.046	44.91	0.27	98.14
4	0.57	0.03	50.52	2.39	0.040	44.91	0.30	98.76
5	0.70	0.03	50.47	3.37	0.037	45.05	0.23	99.89
6	0.61	0.03	50.09	2.92	0.040	45.16	0.27	99.12
7	0.55	0.03	49.71	4.38	0.035	45.07	0.22	99.99
8	0.56	0.03	49.38	3.66	0.040	45.07	0.26	99.00
9	0.57	0.03	48.76	4.55	0.045	45.09	0.20	99.25
10	0.57	0.03	51.44	1.61	0.040	45.02	0.31	99.02
11	0.68	0.03	49.52	4.02	0.047	44.94	0.27	99.51
12	0.52	0.03	49.50	3.42	0.030	45.21	0.21	98.92
13	0.58	0.03	47.59	6.04	0.049	45.10	0.28	99.67
14	0.51	0.03	49.81	2.87	0.040	45.08	0.24	98.58
15	0.55	0.03	49.16	4.59	0.040	45.17	0.22	99.76
16	4.62	0.09	46.09	4.63	0.45	39.03	4.62	99.89
17	4.61	0.11	46.02	2.06	0.55	38.65	6.30	98.30
18	4.20	0.13	45.49	3.21	0.48	39.50	6.08	99.08

Table 2. Contd.

Sample no.	Na_2O	K_2O	CaO	MgO	Fe_2O_3	L.I.O.	I.R. %	Total
19	0.72	0.03	49.71	2.84	0.030	45.47	0.23	99.03
20	0.84	0.03	46.76	7.00	0.028	45.07	0.20	99.93
21	1.06	0.03	49.22	2.91	0.040	45.67	0.27	99.20
22	0.99	0.03	49.02	3.43	0.040	45.41	0.26	99.18
23	1.36	0.03	45.71	6.05	0.052	45.66	0.35	99.21
24	0.84	0.03	50.09	2.48	0.040	45.54	0.25	99.27
25	1.00	0.03	49.21	4.00	0.042	45.32	0.32	99.92
26	1.04	0.03	49.38	2.83	0.040	45.62	0.33	99.27
27	1.05	0.03	49.05	4.02	0.050	45.48	0.32	100.00
28	1.00	0.03	48.32	5.00	0.040	45.29	0.32	100.00
29	1.03	0.03	49.31	3.19	0.040	45.28	0.34	99.22
30	1.13	0.03	49.31	2.46	0.040	45.20	0.33	98.50
31	0.79	0.03	47.34	6.19	0.034	45.37	0.19	99.94
32	1.00	0.03	48.58	3.42	0.030	45.22	0.19	98.47
33	1.00	0.03	48.10	5.31	0.030	45.37	0.15	99.99
34	0.90	0.03	46.32	7.16	0.027	45.38	0.15	99.97
35	1.10	0.03	48.45	3.75	0.040	45.16	0.34	98.87
36	0.80	0.03	48.17	4.32	0.030	45.36	0.19	98.90
37	0.69	0.03	49.18	3.72	0.030	45.44	0.15	99.24
38	0.93	0.03	48.69	4.08	0.030	45.17	0.16	99.09
39	1.00	0.03	48.02	5.37	0.028	45.25	0.15	99.85
40	1.03	0.03	47.38	5.35	0.055	45.62	0.30	99.77
41	0.73	0.03	48.91	3.43	0.040	45.35	0.23	98.72
42	1.10	0.03	48.28	4.63	0.046	45.61	0.24	99.94
43	1.12	0.03	46.67	6.33	0.030	45.63	0.17	99.98
44	0.85	0.03	48.78	3.87	0.030	45.21	0.16	98.93
45	0.92	0.03	48.54	4.38	0.030	45.11	0.20	99.21
46	1.00	0.03	46.90	5.85	0.027	45.69	0.12	99.62

TABLE 3. Chemical analysis showing the trace element concentrations in all samples.

Sample no.	Sr	Pb	Cr	Zn	Co	Cu	Ni
1	523.50	20.26	18.13	16.11	76.74	13.70	55.99
2	540.75	19.96	23.21	33.65	106.76	47.81	69.86
3	546.75	20.49	35.60	20.06	64.41	11.84	60.19
4	578.15	19.12	33.74	13.50	83.24	9.90	63.21
5	531.18	20.50	51.33	10.82	63.15	15.74	32.66
6	574.66	19.22	58.82	18.10	74.66	13.12	53.85
7	493.83	23.73	48.10	11.11	64.82	10.70	53.50
8	515.29	24.22	59.37	16.62	54.62	17.10	44.88
9	599.33	21.66	61.40	12.38	59.34	11.99	41.66
10	652.88	22.76	55.76	18.59	58.09	20.21	43.68
11	548.79	24.47	53.84	14.57	60.27	15.57	44.30
12	508.85	23.28	59.33	18.25	47.92	22.36	43.58
13	609.18	24.28	54.24	18.45	55.31	15.97	53.12
14	562.84	20.90	73.62	23.49	73.62	21.12	44.65
15	589.42	25.46	61.88	9.71	54.87	13.67	47.15
16	402.22	103.67	62.20	11.40	74.64	1.87	41.47
17	387.63	90.72	68.04	10.31	53.61	2.06	51.55
18	375.13	63.85	69.84	9.58	31.93	1.20	43.90
19	500.27	26.96	79.95	18.28	68.53	14.85	42.26
20	488.68	23.82	52.14	14.32	55.55	14.71	34.06
21	554.80	24.36	63.15	24.81	24.81	9.25	53.23
22	510.11	16.53	47.23	33.06	37.79	12.28	47.23
23	450.09	25.81	18.26	14.20	60.41	19.00	40.81
24	532.77	24.44	33.15	9.47	44.99	15.39	33.39
25	593.72	24.01	47.01	26.30	54.17	23.28	25.52
26	547.29	31.20	50.41	16.80	16.80	47.81	36.97
27	512.50	35.92	16.76	16.76	19.16	20.84	37.12
28	435.09	27.26	18.15	11.20	62.21	18.40	40.81
29	535.24	34.92	41.35	20.67	52.83	22.97	44.11
30	544.03	35.18	74.08	23.15	74.08	29.40	37.27
31	390.32	27.18	17.75	10.73	68.89	21.86	33.57

TABLE 3. Contd.

Sample no.	Sr	Pb	Cr	Zn	Co	Cu	Ni
32	437.72	19.83	50.16	20.52	22.80	22.34	28.04
33	510.92	24.57	20.07	8.70	68.39	18.41	33.18
34	471.79	26.84	15.75	6.23	55.25	17.90	24.12
35	406.98	18.02	72.67	63.95	40.70	18.90	25.87
36	408.90	20.08	33.48	11.96	40.65	17.22	29.41
37	440.78	26.78	50.77	16.15	53.08	20.54	34.15
38	428.14	20.04	62.15	6.91	64.45	15.19	27.39
39	422.58	24.30	11.72	7.97	73.83	17.87	55.95
40	506.09	24.39	18.00	10.42	58.37	22.04	34.20
41	457.39	17.66	65.66	13.59	117.74	21.51	50.27
42	403.94	25.18	17.01	9.58	52.86	20.15	28.98
43	458.44	21.38	18.24	7.57	58.40	22.13	39.47
44	433.54	25.82	50.73	18.45	76.10	30.44	37.36
45	405.84	26.43	64.94	11.60	60.30	20.64	35.48
46	488.30	22.36	17.71	7.54	58.21	20.31	31.72

TABLE 4. Correlation matrix of major and trace elements, Karan island, KSA.

Variable	Na_2O	CaO	MgO	Fe_2O_3	L.O.I.	I.R.	Sr	Pb	Cr	Zn	Co	Cu	Ni
Na_2O	1.00	– .58	.32	– .03	.69	.08	– .46	.36	– .31	.05	– .39	.18	– .53
CaO	– .58	1.00	– .89	.18	– . 49	.35	.51	– .12	.40	.25	.16	.06	.44
MgO	.32	– .89	1.00	– .21	.27	– .43	– .41	.08	– .49	– .39	– .04	– .15	– .33
Fe_2O_3	– .03	.18	– .21	1.00	– .04	.78	.44	.08	– .09	.25	.03	.09	.35
L.O.I.	.69	– .49	.27	– .04	1.00	– .10	– .32	.29	– .34	– .18	– .38	.19	– .41
I.R.	.08	.35	– .43	.78	– .10	1.00	.41	.20	.08	.53	– .03	.30	.32
Sr	– .46	.51	– .41	.44	– .32	.41	1.00	.01	.28	.08	.02	– .07	.43
Pb	.36	– .12	.08	.08	.29	.20	.01	1.00	– .10	– .20	– .29	.31	– .22
Cr	– .31	.40	– .49	– .09	– .34	.08	.28	– .10	1.00	.39	– .01	– .09	.01
Zn	.05	.25	– .39	.25	– .18	.53	.08	– .20	.39	1.00	– .12	.19	.09
Co	– .39	.16	– .04	.03	– .38	– .03	.02	– .29	– .01	– .12	1.00	.07	.45
Cu	.18	.06	– .15	.09	.19	.30	– .07	.31	– .09	.19	.07	1.00	– .06
Ni	– .53	.44	– .33	.35	– .41	.32	.43	– .22	.01	.09	.45	– .06	1.00

In general, the original chemical composition of marine sediments depend on the mineralogical composition of the parent rocks under normal conditions. On the other hand both CaO and MgO are associated with the carbonate fraction as could be seen from the strong correlation between them (Table 4). Calcium oxide is the most abundant oxide in all the analyzed reef sediments followed by MgO. CaO is negatively correlated with the MgO, acid soluble carbonate ($CaCO_3$) fraction and the mineralogical composition of the sediments (Table 4). Na_2O has negative correlation with $CaCO_3$ and positive correlation with Fe_2O_3 and insoluble residue indicating its association in the detrital constituents (Fig. 8). K_2O generally occurs in trace amounts together with slight amounts of Fe_2O_3 (Fig. 9).

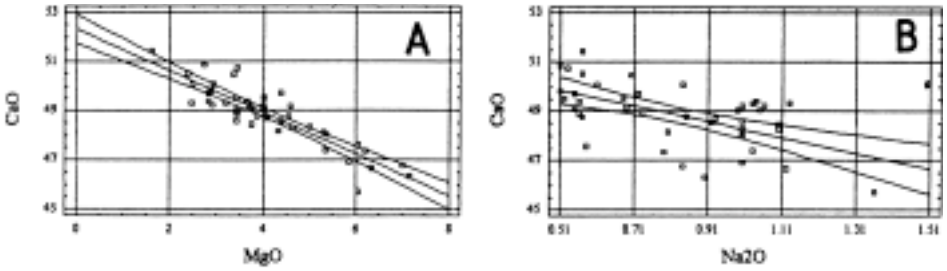

FIG. 8. Correlation between the calcium oxide with the magnesium oxide (A), and the calcium oxide with the sodium oxide (B).

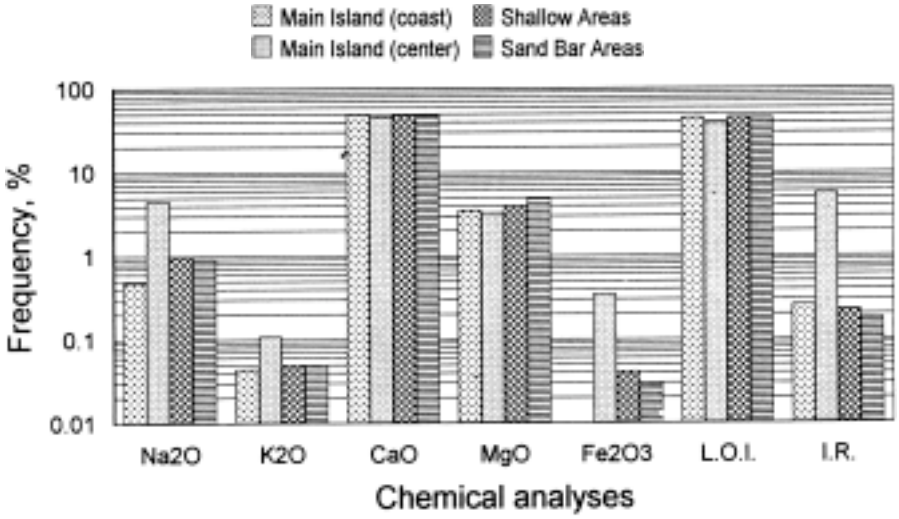

FIG. 9. Major oxides, loss of ignition and insoluble residue distribution in Karan island and surrounding areas.

For the trace elements, the strontium (Sr) is quite common and shows a bimodal distribution in the Keran island (Fig. 10) with a content ranging between 375 ppm and 652 ppm and an average of about 486 ppm. The strontium (Sr) is positively correlated with the calcium oxide and negatively correlated with the sodium oxide (Fig. 11). Estimates of strontium content of modern marine carbonates range from 245 ppm to 600 ppm (Veizer, 1983; Baker and Burns, 1985; Scoffin, 1987). Bathurst (1981) emphasised that

the aragonite and calcite can hold some strontium Sr^{2+}. The free energy of mixing of the strontium Sr^{2+} in the aragonite is greater than in the calcite, thus favoring the aragonite. Graham *et al.* (1981) documented possible Sr/Ca variations in marine water of 15% to 25% during the Cenozoic. The major factor in global geochemistry is the rate of continental weathering processes, which also control atmospheric CO_2 levels, as well as the flux of Sr, Ca, C and other dissolved species of the oceans (Raymo *et al.,* 1988). Strontium has a residence time in the oceans of 4.5 million years and it takes approximately 1000 years to mix the oceans; consequently, Sr concentration in the oceans is uniform (8 ppm) (Tucker and Wright, 1992).

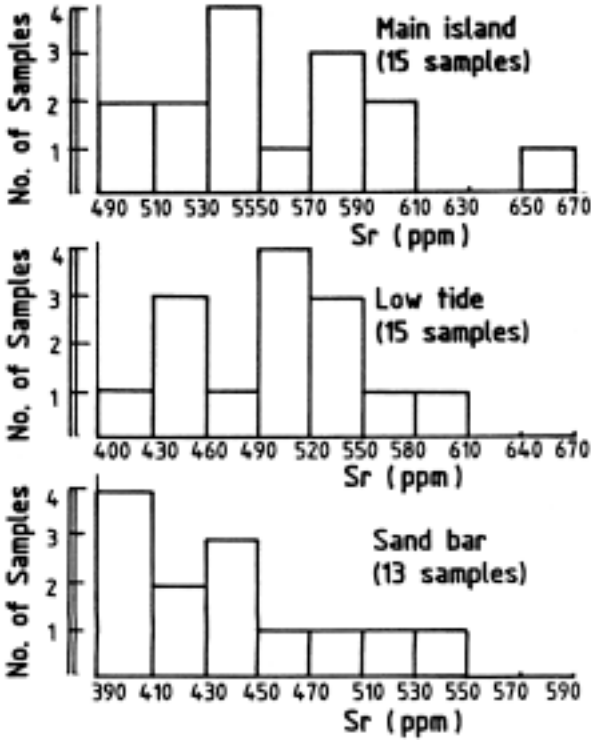

FIG. 10. Histograms showing frequency distribution of Sr (ppm) in Karan island.

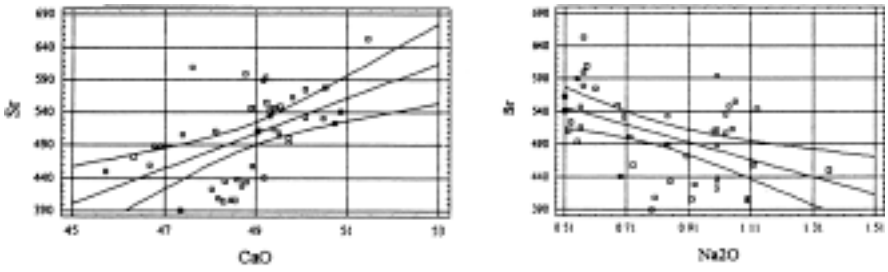

FIG. 11. Correlation coefficient between the calcium oxide with the strontium (A), and the sodium oxide with the strontium (B).

Conclusion

The texture analysis shows one sediment class of a medium grain to coarse grain, moderately to well sorted with occasional very coarse in vegitated areas.

The cumulative curves shows rare suspended particles. While sand population dominant in all samples, long shore currents caused the lateral accretion of carbonate sand spits.

The different results of the Karan island and the Eqah island is due to the tidal currents activity. Although, they are of a similar composition.

Calcite percentage is higher than aragonite as clear in the geochemical analysis, especially on the sand bar area. Whereas, aragonite formed a higher percentage at the main island.

Calcium oxides formed a higher percentage than the iron, potassium, magnesium and sodium oxides, while strontium is common with higher percentage than other trace elements such as lead, chromite, zinc, cobalt, copper and nickel.

The correlation matrix of the calcite oxide show strong relation between the appearance of MgO and CaO oxides. Subsequently, the occurrence of the strontium is a consequence of the existence of the calcite and sodium oxides.

The environment of deposition is apparently of coral reef marine environment.

References

Al-Mansi, A.M., Montello, T.M. and **Al-Momen, A.** (1996) Seasonal profile changes in the western Arabian Gulf. In: *Marine Wildlife Sanctuary for the Arabian Gulf.* Environmental Research and Conservation Following the 1991 Gulf War Oil Spill. NCWCD, Riyadh and Senckenberg Research Institute, Frankfort A.M. (eds: **F. Krupp, A.H. Abuzinada** and **I.A. Nader;** pp. 33-290.

Baker, P.A. and **Burns, S.J.** (1985) Occurrence and formation of dolomite in organic-rich continental margin sediments: *Am. Assoc. Petrol. Bull.* **69:** 1917-1930.

Basaham, A.S. and **El-Sayed, M.A.** (1998) Distribution and phase association of some major and trace elements in the Arabian Gulf sediments. *Estuarine, Coastal and Shelf Science* **46:** 185-194.

Basyoni, M.H. and **Al-Mansi, A.M.A.** (19930 The grain-size trends on a recent reef island, Red Sea, Saudi Arabia. *Arab. Gulf J. Scient.* **11**(2): 155-168.

Bathurst , R.G.C. (1981) *Developments in Sedimentology.* Elsevier Scientific Publication Company, Oxford, New York, pp. 242-243.

Evamy, B.D. (1973) The precipitation of aragonite and the alteration to calcite on the Trucial Coast of the Persian Gulf, in: **B.H. Purser,** ed., *The Persian Gulf.* Springer-Verlag, New York, pp. 329-341.

Folk, R.L. and **Ward, W.C.** (1957) Brazos River Bar; A study in the significance of grain size parameters, *Jour. Sed. Petrology*, **27:** 3-26.

——— (1968) *Petrology of Sedimentary Rocks:* Austin, Texas, Hemphill's Book Store, 170 p.

Fryberger, S.G., Al-Sari, A.M. and **Clisham, T.J.** (19830 Eolian dune, interdune, sand sheet, and siliciclastic sabkha sediments of an offshore prograding sand sea, Dhahran Area, Saudi Arabia. *AAPG Bulletin*, **67**(2): 280-332.

Graham, D.W., Bender, M.L., Williams, D.F. and **Keighwin, L.D.** (1981) Strontium to calcium ratio in Cenozoic planktonic foraminifera. *Geochim. Cosmochim. Acta.* **46:** 1281-1292.

Hughes, Clarks, M.W. and **Keij, A.J.** (1973) Organisms as producers of carbonate sediment and indicator of environment in the southern Persian gulf. In: *The Persian Gulf.* ed. by **B.H. Purser,** pp. 33-56.

Hunter, J.R. (1986) The physical oceanography of the Arabian Gulf: a review and theoretical interpretation

of previous observations. In: *The First Arabian Gulf Conference on Environmental and Pollution* (**A. Al-Adwani, A. Al-Ageel** and **R. Halwogy,** eds). Alden Press, Kuwait, pp. 1-23.

Javor, B.J. (1985) Nutrients and ecology of the western salt and exportadora de sal saltern brines. In: *Sixth Symposium on Salt,* **V.I.,** pp. 195-206.

Khalaf, F., Al-Bakri, D. and **Al-Ghadban, A.** (1984) Sedimentological characteristics of the surficial sediments of the Kuwaiti marine environment, northern Arabian Gulf. *Sedimentology,* **31:** 531-545.

McCave, I.N. (1978) Grain-size trends and transport along beaches. Example from Eastern England. *Mar. Geol.* **28:** 43-51.

Milliman, J.D. (1989) Sea level: past, present, and future. *Oceanus,* **32**(2): 40-44.

Moshrif, M.A. (1987) *Principles of Sedimentology.* University Libraries, King Saud University, 710 p. (Arabic Edition).

Purser, B.H. and **Seibold, E.** (1973) The principal environmental factors influencing Holocene sedimentation and diagenesis in the Persian Gulf. In: *The Persian Gulf,* **B.H. Purses,** ed., pp. 1-90.

Raymo, M.E., Ruddiman, W.F. and **Froelich, P.N.** (1988) Influence of late Cenozoic mountain building on ocean geochemical cycles. *Geology* **16:** 649-653.

Scoffin, T.P. (1987) An Introduction to Carbonate Sediments and Rocks. Blackie Co. Pub., New York, 274 p.

Sheppard, C.R.C. and **Sheppard, A.L.S.** (1991) Corals and coral communities of Arabia. *Fauna of Saudi Arabia* **12:** 3-17.

Sirag, A. (1984) Climatological features of Saudi Arabia. *Fauna of Saudi Arabia,* **6:** 32-52.

Tucker, M.E. and **Wright, V.P.** (1992) *Carbonate Sedimentology,* Blackwell Scientific Publications. London, Chap. 3, pp. 90-96.

Veizer, J. (1983) Chemical diagenesis of carbonates: Theory and application of trace elements technique; in: **Wallance, M.C.,** Origin of dolomitization on the Barbwire Terrace, Canning Basin Western Australia. *Sedimentology,* **37:** 105-122.

رسوبيات وجيوكيميائية جزيرة كاران ، الخليج العربي المملكة العربية السعودية

محمد بن حسين بسيوني
كلية علوم الأرض ، جامعة الملك عبد العزيز
جـــدة – المملكة العربية السعودية

المستخلص . جزيرة كاران عبارة عن شعاب مرجانية تتشكل أساسًا من الكالسايت والأراجونايت . وتغطي الجزيرة بواسطة حبيبات رملية كربوناتية متوسطة إلى خشنة هيكلية وغير هيكلية ذات أصل بحري مع ندرة وجود الجزئيات الطينية المحمولة مع العواصف الريحية . إن توزيع حجم الحبيبات للرسوبيات يعتبر أحادي التماثل ورديئة إلى جيدة الفرز .

وبناءً على نتائج الأشعة السينية والتحاليل الكيميائية للكالسايت والأراجونايت اتضح أن أصل حبيبات الرمل على الجزيرة هو من الشعاب المرجانية .